Physics Letters B 783 (2018) 234–240

Contents lists available at ScienceDirect

Physics Letters B

www.elsevier.com/locate/physletb

# Competition between delta isobars and hyperons and properties of compact stars

Jia Jie Li [a,*], Armen Sedrakian [b], Fridolin Weber [c,d]

[a] Institute for Theoretical Physics, J.W. Goethe University, D-60438 Frankfurt am Main, Germany
[b] Frankfurt Institute for Advanced Studies, D-60438 Frankfurt am Main, Germany
[c] Department of Physics, San Diego State University, 5500 Campanile Drive, San Diego, CA 92182, USA
[d] Center for Astrophysics and Space Sciences, University of California at San Diego, La Jolla, CA 92093, USA

ARTICLE INFO

*Article history:*
Received 10 March 2018
Received in revised form 20 May 2018
Accepted 21 June 2018
Available online 28 June 2018
Editor: W. Haxton

*Keywords:*
Equation of state
Dense matter
Delta resonance
Compact stars

ABSTRACT

The Δ-isobar degrees of freedom are included in the covariant density functional (CDF) theory to study the equation of state (EoS) and composition of dense matter in compact stars. In addition to Δ's we include the full octet of baryons, which allows us to study the interplay between the onset of delta isobars and hyperonic degrees of freedom. Using both the Hartree and Hartree–Fock approximation we find that Δ's appear already at densities slightly above the saturation density of nuclear matter for a wide range of the meson–Δ coupling constants. This delays the appearance of hyperons and significantly affects the gross properties of compact stars. Specifically, Δ's soften the EoS at low densities but stiffen it at high densities. This softening reduces the radius of a canonical $1.4M_\odot$ star by up to 2 km for a reasonably attractive Δ potential in matter, while the stiffening results in larger maximum masses of compact stars. We conclude that the hypernuclear CDF parametrizations that satisfy the $2M_\odot$ maximum mass constraint remain valid when Δ isobars are included, with the important consequence that the resulting stellar radii are shifted toward lower values, which is in agreement with the analysis of neutron star radii.



## 1. Introduction

Compact stars are unique laboratories for studies of dense hadronic matter [1–6]. The hadronic core of a compact star extends from half up to a few times the nuclear saturation density $\rho_0$. In the high-density region of the core a number of exotic degrees of freedom are expected to appear in addition to nucleons. Possible new constituents of matter include hyperons [7–30], delta isobars [8,9,31–41], and deconfined quark matter [46–65]. The details of the composition of compact stars at high densities are not fully understood yet. The current observational programs focusing on neutron stars combined with the nuclear physics modeling of their interiors are aimed at resolving the puzzles associated with their EoS and interior composition.

Although the appearance of Δ's in neutron star matter was conjectured long ago [8,31] there has been much less research on their properties in the intervening years as compared to hyperons and quark matter. This may partially be a consequence of Ref. [9] where Δ's were found to appear at densities that are much larger than the typical central densities of neutron stars. Thus, Δ's have been considered largely unimportant in neutron star astrophysics.

Recently, a number of studies of Δ's in neutron star matter appeared which were conducted within the CDF theory in the Hartree approximation, i.e., the so-called relativistic mean-field model [28,29,34–41]. Some of these studies ignore hyperons in order to isolate the effects Δ isobars have on the nucleonic EoS and neutron star properties by choosing a particular set (in some cases several sets) of meson–Δ coupling constants [29,34,39,41]. The universal coupling scheme is typically adopted in these studies. In analogy to hyperons, the Δ degrees of freedom were found to soften the EoS of neutron star matter and to reduce the maximum mass of a compact star. However, a simultaneous treatment of hyperons and Δ's appears to be mandatory in order to assess the overall effect of these new degrees of freedom on dense matter and the gross properties of compact stars.

The Δ degrees of freedom in nuclear dynamics have been studied in a number of alternative settings. Δ's play an important role

* Corresponding author.
*E-mail addresses:* jiajieli@itp.uni-frankfurt.de (J.J. Li), sedrakian@fias.uni-frankfurt.de (A. Sedrakian), fweber@sdsu.edu (F. Weber).

https://doi.org/10.1016/j.physletb.2018.06.051

in the studies of nucleon–pion–$\Delta$ dynamics, which resum the RPA diagrams including $\Delta$-hole loops with the $\Delta$-hole vertex given by $g'_{N\Delta}$ Landau–Migdal parameter [42–44]. These studies are mainly focused on the pion propagator and dispersion (condensation) in nuclear matter. More recently, $\Delta$'s were included in the studies of nuclear matter in the chiral approach where the nuclear density functional is arranged in powers of small parameters (e.g. number of derivatives of the pion field) and $\Delta$'s appear in virtual states [45].

The principal aim of this work is to explore, in great detail, the competition between $\Delta$ isobar and hyperon populations in dense matter, and to study the impact of $\Delta$ populations on the properties of compact stars such as masses and radii. For that purpose we carry out a detailed analysis of the parameter space of the meson–$\Delta$ coupling values within the CDF theory at the relativistic Hartree and Hartree–Fock level.

This work is organized as follows. In Sec. 2 we outline the CDF model and its parametrizations. Section 3 presents our results for the EoS of dense matter and its composition. The global properties of compact stars and their internal structures are discussed in this section as well. Finally, a summary of our results is provided in Sec. 4.

## 2. Theoretical model

### 2.1. CDF model for stellar matter

We start with a brief outline of our theoretical framework, which is based on the CDF theory treated in the Hartree and Hartree–Fock approximations. The Lagrangian density of the model is given by

$$\mathscr{L} = \mathscr{L}_B + \mathscr{L}_m + \mathscr{L}_{\rm int} + \mathscr{L}_l, \tag{1}$$

where the first term $\mathscr{L}_B$ is the Lagrangian of free baryonic fields $\psi_B$, with index $B$ labeling the spin-1/2 baryonic octet, which comprises nucleons $N \in \{n, p\}$, hyperons $Y \in \{\Lambda, \Xi^{0,-}, \Sigma^{+,0,-}\}$, and the spin-3/2 zero-strangeness quartet $\Delta \in \{\Delta^{++,+,0,-}\}$. Note that the $\Delta$'s are treated as Rarita–Schwinger particles [66]. The second term $\mathscr{L}_m$ represents the Lagrangian of free meson fields $\phi_m$, which are labeled according to their parity, spin, isospin and strangeness. In the present model we include the isoscalar–scalar meson $\sigma$, which mediates the medium-range attraction between baryons, the isoscalar–vector meson $\omega$, which describes the short range repulsion, the isovector–vector meson $\rho$, which accounts for the isospin dependence of baryon–baryon interactions, and the $\pi$ meson which accounts for the long-range baryon–baryon interaction and the tensor force. The two hidden-strangeness mesons, $\sigma^*$ and $\phi$, describe interactions between hyperons. The interaction between the baryons and mesons is described by the third term $\mathscr{L}_{\rm int}$ which has the generic form

$$\mathscr{L}_{\rm int} \equiv g_{mB}\tau_B\bar{\psi}_B\Gamma_m\varphi_m\psi_B, \tag{2}$$

where $g_{mB}$ is the meson–baryon coupling constant, $\tau_B \in \{1, \boldsymbol{\tau}\}$ is the isospin matrix and $\Gamma_m \in \{1, \gamma_\mu, \gamma_5\gamma_\mu, \sigma_{\mu\nu}\}$ is the relevant (Dirac-matrix) vertex. Finally, the last term $\mathscr{L}_l$ describes the contribution from free leptons; we include electrons ($e^-$) and muons ($\mu^-$) and neglect the neutrinos which are irrelevant at low temperatures.

Starting from Eq. (2) we carry out the standard procedure for obtaining the density functional in CDF theories. This amounts to finding the equations of motions from the Euler–Lagrange equations of the theory, which for the baryon octet and leptons have the form of the Dirac equation, whereas for the $\Delta$ decuplet are given by the Rarita–Schwinger equation. The equations of motion for meson in the mean-field approximation take the form of Klein–Gordon equation. Each of the baryon self-energies is then decomposed in the Dirac space according to

$$\Sigma(k) = \Sigma_S(k) + \gamma_0\Sigma_0(k) + \boldsymbol{\gamma}\cdot\hat{\boldsymbol{k}}\Sigma_V(k) \tag{3}$$

where $\Sigma_S$, $\Sigma_0$ and $\Sigma_V$ are the scalar, time and space components of the vector self-energies and $\hat{\boldsymbol{k}}$ is a unit vector along $\boldsymbol{k}$. The energy density functional is then generated by evaluating the baryon self-energies $\Sigma(k)$ in the Hartree (RMF) or Hartree–Fock (RHF) approximations [67–70]. The detailed expressions for self-energies are given, for instance, in Refs. [41,71]. Note that the pion-exchange and the tensor couplings of vector mesons to baryons contribute only to the Fock self-energies. In $\beta$-equilibrium the chemical potentials of the particles are related to each other by

$$\mu_B = b_B\mu_n - q_B\mu_e, \tag{4}$$

where $b_B$ and $q_B$ denote the baryon number and electric charge of baryon species $B$, and $\mu_n$ and $\mu_e$ are the chemical potentials of neutrons and electrons, respectively. This, together with the field equations and charge neutrality condition allows us to determine the EoS and composition of matter for any given net baryonic density $\rho$ at zero temperature self-consistently.

Once the EoS is determined, the integral parameters, in particular the mass and the radius, of a compact star of given central density can be computed from the Tolman–Oppenheimer–Volkoff (TOV) equations [72,73]. To do so we match smoothly our EoS to an EoS of the inner and outer crusts [74,75] at the crust–core transition density $\rho_0/2$, where $\rho_0$ denotes the saturation density of ordinary nuclear matter.

### 2.2. Meson–baryon couplings

We now turn to the procedure of choosing the appropriate values of the coupling constants $g_{m\Delta}$ between the mesons and baryons. These have to be fitted to the experimental (empirical) data of nuclear and hypernuclear systems. In the purely nucleonic sector the meson–nucleon ($mN$) couplings are given by $g_{mN}(\rho) = g_{mN}(\rho_0)f_{mN}(x)$, where $x = \rho/\rho_0$. For the isoscalar channel, one has

$$f_{mN}(x) = a_m\frac{1 + b_m(x + d_m)^2}{1 + c_m(x + d_m)^2}, \quad m = \sigma, \omega, \tag{5}$$

which is subject to constraints $f_{mN}(1) = 1$, $f''_{mN}(0) = 0$ and $f''_{\sigma N}(1) = f''_{\omega N}(1)$. The density dependence for the isovector channels is taken in an exponential form[1]

$$f_{mN}(x) = e^{-a_m(x-1)}, \quad m = \rho, \pi. \tag{6}$$

In the hypernuclear sector, as usual, the vector meson–hyperon couplings are given by the SU(3) flavor symmetric quark model [11,76] whereas the scalar meson–hyperon couplings are determined by their fitting to empirical hypernuclear potentials. We note that the isovector couplings are non-universal and, for example, values $g_{\rho\Sigma}/g_{\rho N} \simeq 1/4$–$1/3$ are required to describe the $\Sigma$-atom [77].

[1] For the PKO3 interaction used in this study the masses (in MeV) of nucleon, $\sigma$-, $\omega$-, $\rho$- and $\pi$-mesons are 938.9, 525.6677, 783, 769, 138. The coupling constants at the saturation $\rho_0 = 0.153$ fm$^{-3}$ are $g_\sigma = 8.8956$, $g_\omega = 10.8027$, $g_\rho = 2.0302$ and $f_\pi = 0.3929$; the remaining parameters, which describe the density-dependence of couplings can be found in Table 1 of Ref. [85].

**Table 1**
The parameters of symmetric nuclear matter at saturation density and the masses and radii of hypernuclear stars, predicted by the hypernuclear CDF theory with PKO3 and DD-ME2 parametrizations. Upper panel: the saturation density $\rho_0$ (fm$^{-3}$), binding energy $E_B$ (MeV), compression modulus $K$ (MeV), symmetry energy $J$ (MeV) and its slope $L$ (MeV), the Dirac mass $M_D^*$ (in units of nucleon mass $M$), and the Landau mass $M_L^*$ ($M$) for symmetric nuclear matter. Lower panel: The mass $M_{\max}$ (in solar units), radius $R_{\max}$ (km) and central density $\rho_{\max}$ (fm$^{-3}$) of the maximum-mass star, the threshold density $\rho_Y^c$ (fm$^{-3}$) for hyperons $\Lambda$ and $\Xi^-$, the radius $R_{1.4}$ (km) and central density $\rho_{1.4}$ (fm$^{-3}$) for a canonical $1.4M_\odot$ neutron star.

| CDF | Symmetric nuclear matter | | | | | | |
|---|---|---|---|---|---|---|---|
| | $\rho_0$ | $E_B$ | $K$ | $J$ | $L$ | $M_D^*$ | $M_L^*$ |
| PKO3 | 0.153 | −16.04 | 262.44 | 32.99 | 82.99 | 0.59 | 0.72 |
| DD-ME2 | 0.152 | −16.14 | 251.15 | 32.31 | 51.27 | 0.57 | 0.63 |
| | Hypernuclear matter | | | | | | |
| | $M_{\max}$ | $R_{\max}$ | $\rho_{\max}$ | $\rho_\Lambda^c$ | $\rho_\Xi^c$ | $R_{1.4}$ | $\rho_{1.4}$ |
| PKO3 | 2.00 | 11.82 | 0.96 | 0.33 | 0.48 | 13.96 | 0.31 |
| DD-ME2 | 2.00 | 11.83 | 0.93 | 0.34 | 0.38 | 13.22 | 0.34 |

Let us focus now on the range of the meson–$\Delta$ couplings. No consensus has been reached yet on the magnitude of the $\Delta$ potential in nuclear matter. The phenomenological model analyses of the scattering of electrons and pions off nuclei and photoabsorption [78–81] indicate that the $\Delta$ isoscalar potential $V_\Delta$ should be in the range [37]

$$-30\ \text{MeV} + V_N(\rho_0) \lesssim V_\Delta(\rho_0) \lesssim V_N(\rho_0), \tag{7}$$

where $V_N = \Sigma_{0,\omega(\sigma)} + \Sigma_{S,\sigma(\omega)}$ is the nucleon isoscalar potential. The studies of $\Delta$ production in heavy-ion collisions [82–84] suggest a less attractive potential [29],

$$V_N(\rho_0) \lesssim V_\Delta(\rho_0) \lesssim 2/3 V_N(\rho_0). \tag{8}$$

Below, we will use instead of $g_{m\Delta}$ the ratio $R_{m\Delta} = g_{m\Delta}/g_{mN}$. The isoscalar potential of the $\Delta$ isobars in symmetric nuclear matter at saturation density is thus given by

$$V_\Delta(\rho_0) = R_{\omega\Delta}\Sigma_{0(S),\omega}(\rho_0) + R_{\sigma\Delta}\Sigma_{S(0),\sigma}(\rho_0). \tag{9}$$

The isovector meson–$\Delta$ couplings are largely unknown. It has been found that the critical density of the onset of $\Delta$'s is most sensitive to the ratio $R_{\rho\Delta}$ [37,39]. In our numerical study we use two representative parametrizations of the nucleonic CDF theory based on the density-dependent meson–baryon couplings, specifically the relativistic Hartree–Fock PKO3 parametrization [85] and the relativistic Hartree DD-ME2 parametrization [86]. Both parametrizations describe successfully the properties of finite nuclei. We will use the extensions of these models to the hypernuclear sector as given in Ref. [71]. In this work the meson–hyperon couplings have been chosen to: (a) reproduce the empirical potentials of hyperons in nuclear matter deduced from nuclear structure calculation and (b) produce heavy $2M_\odot$ compact stars [87]. In Table 1 we list the key parameters of symmetric nuclear matter and some properties of hyperonic stars predicted by the two models. Note that the combined analysis of terrestrial experiments and astrophysical observations [6] predict values for the symmetry energy $J = 31.7 \pm 3.2$ MeV and its slope $L = 58.7 \pm 28.1$ MeV at saturation density. The $J$ value predicted by both parametrizations are compatible with the central value of 32 MeV, while the value of $L$ predicted by PKO3 is located at the upper bound of the preferred range.

## 3. Results and discussions

In this section we investigate the competition between $\Delta$ isobars and hyperons in dense stellar matter and their effect on the properties of compact stars. In a first step, we will analyze the EoS of stellar matter with $\Delta$'s for selected sets of $R_{m\Delta}$ values, which are motivated by the constraints shown in Eqs. (7) and (8); note that the value of the potential $V_\Delta$ does not fix any of the couplings, rather it provides a relation between $R_{\omega\Delta}$ and $R_{\sigma\Delta}$. This illustrates the general features that emerge when $\Delta$ isobars are included. In the second step, we construct the EoS and the associated stellar models for a continuum of meson–$\Delta$ couplings which span the complete parameter space. This provides insight into the dependence of the stellar parameters on $R_{m\Delta}$, which, in turn, permits us to narrow down the meson–$\Delta$ parameter space using the astrophysical constraints.

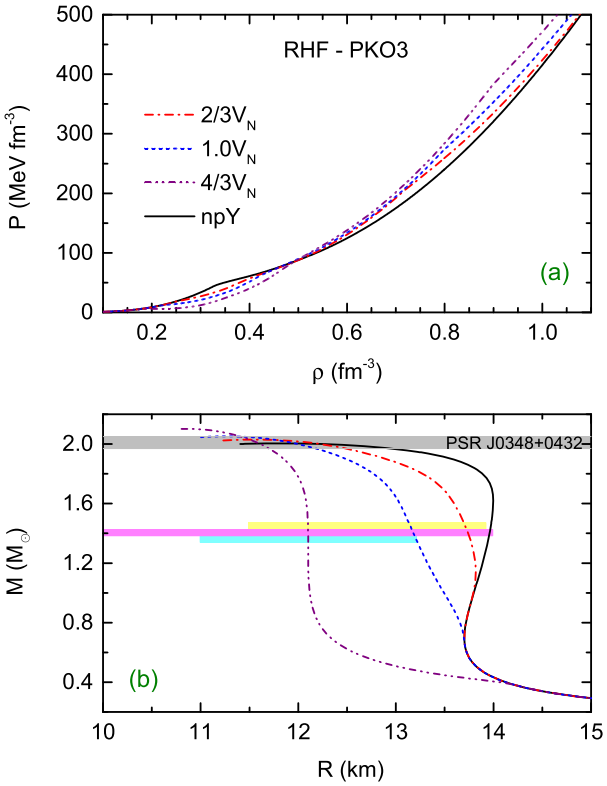


**Fig. 1.** Effects of $\Delta$-isobars on the EoS and mass–radius relation of compact stars. (a) EoSs for different $\Delta$ potential depths $V_\Delta(\rho_0) = (1 \pm 1/3)V_N(\rho_0)$, $npY$ denotes the hyperonic matter, (b) the corresponding mass–radius relations. The gray shading indicates the mass of PSR J0348+0432. The yellow, pink, and cyan shading indicate the radius range of canonical $1.4M_\odot$ neutron stars set by Refs. [88–90]. Notice that the ordering of the EoSs according to their stiffness depends on the density interval. The $\omega$–$\Delta$ coupling constants are fixed as 1.1, while the $\sigma$–$\Delta$ coupling constants are adjusted to the potential depths $V_\Delta(\rho_0)$, which corresponds to $R_{\sigma\Delta} = 1.075 \pm 0.125$. The results are calculated for the RHF parametrization PKO3. (For interpretation of the colors in the figure(s), the reader is referred to the web version of this article.)

### 3.1. Illustrative cases

We start with several illustrative examples which are constructed as follows: (a) the $R_{\omega\Delta}$ parameter is kept fixed at a value of 1.1, which leads to the largest masses of compact star for our parameter space (to be discussed in Fig. 3 below); (b) all isovector meson couplings are set equal to the meson–nucleon coupling; (c) the potential $V_\Delta$ is varied within the bounds set by Eqs. (7) and (8) by tuning the $R_{\sigma\Delta}$ parameter.

In Fig. 1(a) we show the EoS of $\Delta$-admixed-hypernuclear ($npY\Delta$) matter for three values of the isoscalar potential $V_\Delta(\rho_0)$. For comparison, we also show the case of matter without $\Delta$'s, i.e., $npY$ matter. The corresponding mass–radius relations of compact-star models computed for these EoS are shown in Fig. 1(b). In the

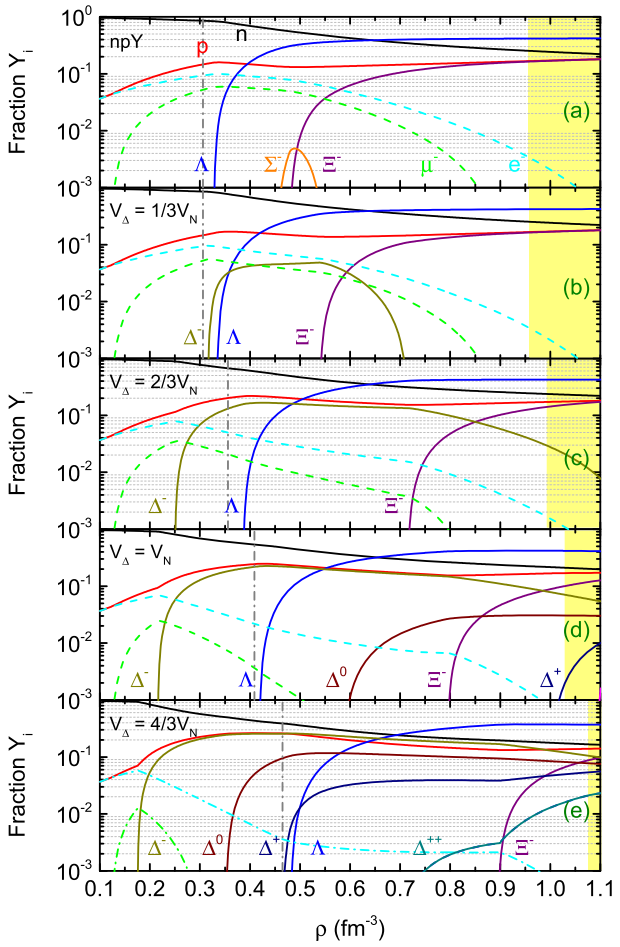


**Fig. 2.** Particle fractions in $npY$ (panel a) and $npY\Delta$ (panels b, c, d and e) matter. The $\Delta$ potential depths are $V_\Delta = 1/3V_N$ (b), $2/3V_N$ (c), $V_N$ (d) and $4/3V_N$ (e). The thick vertical lines indicate the central density of the respective canonical $1.4M_\odot$ neutron star, the yellow shadings indicate densities beyond the maximum mass configurations. The results are calculated by using the RHF parametrization PKO3.

case of $npY$ matter the abrupt change in the slope of the pressure at baryonic density $\rho \simeq 0.33$ fm$^{-3}$ is the result of the onset of hyperons in matter. It is seen that if $\Delta$'s are included in the composition, the EoS is softened at low and stiffened at high densities. This is the more pronounced the deeper the $V_\Delta(\rho_0)$ potential.

These modifications in the EoS affect the mass–radius relations of neutron-star models as depicted in Fig. 1(b). It is seen that accounting for $\Delta$'s reduces the radii of models from their values obtained for hypernuclear and nuclear matter EoS. This is a consequence of the *softening of the EoS* at low to intermediate baryonic densities. Note that the $\Delta$'s may appear already at densities slightly above the nuclear saturation density, which implies that even low-mass ($\simeq M_\odot$) compact stars can be affected by $\Delta$ populations. As expected, the larger the $V_\Delta(\rho_0)$ potential, the larger is the observed shift in the radius. For example, for $V_\Delta(\rho_0) = 4/3V_N(\rho_0)$ the radius of a canonical $1.4M_\odot$ neutron star is about 2 km smaller than the radius of its purely hyperonic or nucleonic counterpart. At the same time, $\Delta$'s lead to marginally greater maximum masses of compact stars, because of the *stiffening of the EoS* in the high-density region. The deeper the potential $V_\Delta(\rho_0)$ the larger the star's maximum mass.

Fig. 2 shows the particle fractions for several selected values of the $V_\Delta(\rho_0)$ potential. In the case of hyperonic matter without $\Delta$'s, shown in Fig. 2(a), the first hyperon to appear is the $\Lambda$, which is followed by the $\Xi^-$ hyperon. The $\Sigma^-$ hyperons appear only briefly, because they are disfavored due to their repulsive potential at nuclear saturation density. This sequence of hyperon thresholds is consistent with the recent hypernuclear CDF computations of Refs. [16,26,28,30]. In the cases when $\Delta$'s are taken into account the following new features are observed: (1) The $\Delta$-threshold density could be at much lower density than that for the first hyperon (i.e., the $\Lambda$). The larger the potential $V_\Delta^{(N)}$ the lower the onset threshold for $\Delta$'s. (2) The first $\Delta$ isobar to appear is the $\Delta^-$, which eliminates the $\Sigma^-$ entirely and significantly shifts the threshold for the $\Xi^-$; the threshold of the $\Lambda$ hyperon is also shifted but to a lesser extent. (3) In the case of a strongly attractive potential $V_\Delta \leq V_N$, the $\Delta^{0,+}$ resonances appear at intermediate to high densities, in addition to the $\Delta^-$. (4) Electric charge neutrality, maintained by baryons and leptons, implies that the onset of the $\Delta^-$ not only shifts the threshold of $\Xi^-$ hyperons, but leads also to a depletion of the negatively charged lepton population, especially that of muons. (5) For $V_\Delta \geq 2/3V_N$ the threshold for the onset of $\Delta$'s is reached in a canonical $1.4M_\odot$ neutron star. Furthermore, the central density of the maximum-mass star is larger by about 0.1 fm$^{-3}$ than in the absence of $\Delta$'s.

**Table 2**
The threshold densities (in fm$^{-3}$) for the onset of direct Urca processes in $npY$ matter (rows 1 and 3) and in $npY\Delta$ matter with $V_\Delta(\rho_0) = V_N(\rho_0)$ (rows 2 and 4). No entry means that the process is forbidden. The rows 1 and 2 correspond to PKO3, and rows 3 and 4 to the DD-ME2 parametrizations. The thresholds (from left to right) corresponds to the following processes: $n \to p + e^- + \bar{\nu}_e$, $\Delta^- \to \Lambda + e^- + \bar{\nu}_e$, $\Lambda \to p + e^- + \bar{\nu}_e$, and $\Xi^- \to \Lambda + e^- + \bar{\nu}_e$.

| CDF | Composition | $\rho_n^{\rm DU}$ | $\rho_{\Delta^-}^{\rm DU}$ | $\rho_\Lambda^{\rm DU}$ | $\rho_{\Xi^-}^{\rm DU}$ |
|---|---|---|---|---|---|
| PKO3 | $npY$ | 0.282 | – | 0.329 | 0.536 |
| | $npY\Delta$ | 0.271 | 0.431 | 0.458 | – |
| DD-ME2 | $npY$ | – | – | 0.341 | 0.382 |
| | $npY\Delta$ | – | 0.358 | 0.366 | – |

The inclusion of the $\Delta$-isobars in the EoS of neutron stars can impact their cooling through modifications of the direct Urca (DU) neutrino emissivities in the star's core. The onsets densities of the electronic versions of DU processes in purely $npY$ and $npY\Delta$ matter are listed in Table 2. We recall that for $npY$ matter, the nucleonic DU process ($n \to p + e^- + \bar{\nu}_e$) occurs only for the PKO3 parametrization, while the hyperonic DU processes operate for both PKO3 and DD-ME2 parametrizations as soon as hyperon states are populated [71]. In $npY\Delta$ matter the early appearance of the $\Delta^-$ causes a significant increase in the proton ($p$) fraction but a decrease in the $e^-$ fraction (see Fig. 2). As a result, the onset of the nucleonic DU process is slightly shifted toward lower densities for the PKO3 parametrization. This also results in a delay in the onset of the $\Lambda \to p + e^- + \bar{\nu}_e$ process as the density increases. The $\Delta^- \to \Lambda + e^- + \bar{\nu}_e$ process proceeds for both parametrizations shortly after the $\Lambda$'s appear, which occurs for stars with masses $M \geq 1.5M_\odot$. The $\Xi^- \to \Lambda + e^- + \bar{\nu}_e$ process is absent at high density due to the very low fraction of leptons. Our speculations above show that the inclusion of $\Delta$'s may cause substantial modifications in the rates at which neutrinos are emitted from neutron stars. It will be worthwhile to explore these modifications in numerical cooling simulations.

### 3.2. Meson–$\Delta$ coupling space

Having established some general trends, we would now like to explore the parameter space in a more systematic manner. We will still keep the isovector meson–$\Delta$ couplings in accord with the universal scheme, i.e., $R_{\rho(\pi)\Delta} = 1.0$. Instead of having $R_{\omega\Delta} = 1.1$ we will now allow for variations of $R_{\omega\Delta} \in [0.8; 1.6]$ and $R_{\sigma\Delta} - R_{\omega\Delta} \in [-0.20; 0.20]$. As we will see below, such a range captures the

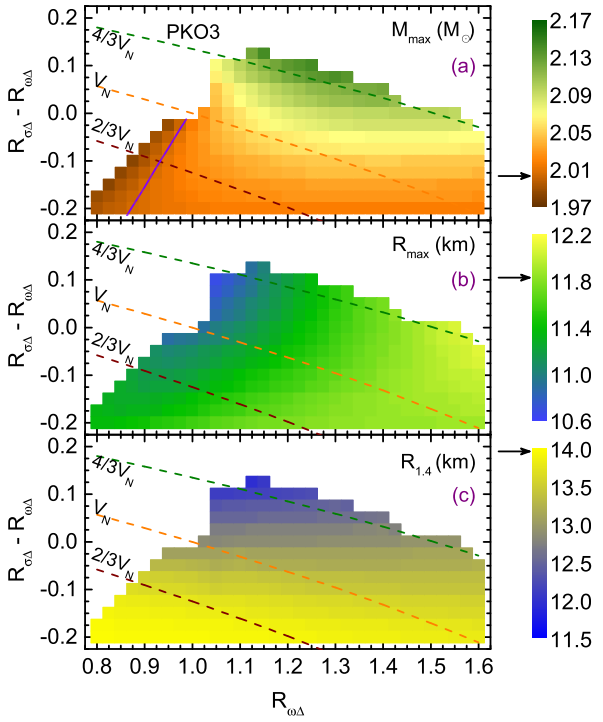


**Fig. 3.** Contour plots for the gross properties of compact stars in the parameter space spanned by $R_{\omega\Delta}$ and $(R_{\sigma\Delta} - R_{\omega\Delta})$. Shown are the: (a) maximum mass, (b) radius of the maximum mass star, and (c) radius of a canonical $1.4M_\odot$ star. The dashed lines show the constant values of the potential $V_\Delta = (1 \pm 1/3)V_N$. The solid line in the lower-left corner of panel (a) means that the configurations contain $\Delta$'s but have a mass equal to the purely hyperonic star. The white areas indicate coupling sets for which no physical solutions exist. The mass and radii for purely hyperonic matter are marked by horizontal arrows pointing at the labels. To obtain these results we used the RHF parametrization PKO3. Analogous contour plots for relativistic mean-field models were first obtained in Ref. [28].

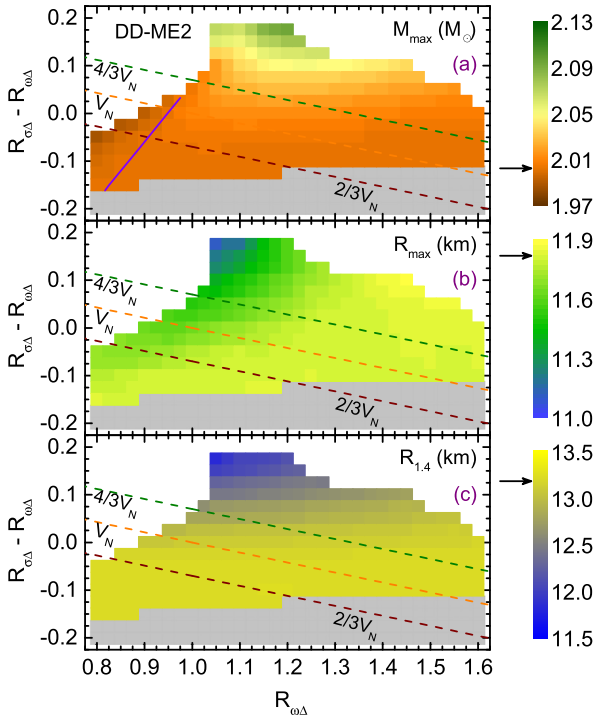


**Fig. 4.** Same as Fig. 3, but for the RMF parametrization DD-ME2. The grey pixels show areas where no $\Delta$-isobars are populated.

most interesting region of the parameter space spanned by the masses and radii of the models.

The three panels in Fig. 3 show the value of the maximum-mass star, the radius of this star, and the radius of a canonical $1.4M_\odot$ star, computed for the PKO3 parametrization. Fig. 4 shows the same quantities but computed for the DD-ME2 parametrization. The white areas indicate the range of couplings for which the EoS is unphysical due to either a negative Dirac baryon mass or a non-monotonic pressure. The grey pixels indicate that no $\Delta$-isobars are populated. The lines of constant values of the potential $V_\Delta = (1 \pm 1/3)V_N$ are also shown.

Figs. 3 and 4 display some common features on which we comment first; we will return to differences below. It is seen that (a) the maximum masses increase when the couplings $R_{m\Delta}$ are increased, i.e., when moving from the lower-left corner to the right. For $R_{m\Delta} \leq 1.0$, i.e., when $\Delta$'s interact weaker than nucleons, the stellar masses are close or slightly below the $2M_\odot$ limit (i.e., the purely hyperonic case). For the parameter space considered here, the stellar masses are consistent with the current observational limits on pulsar masses. The heaviest stars appear when both $V_\Delta$ is most attractive and the difference $(R_{\sigma\Delta} - R_{\omega\Delta})$ is largest. (b) The smallerst radii of the maximum-mass stars are located in the region where $R_{\omega\Delta} \sim 1.0$ and $R_{\sigma\Delta} \sim 1.1$, i.e., the most massive compact stars are not automatically also the most compact ones. Quite generally, the radii of stars containing $\Delta$'s in their cores are smaller than the radii of their nucleonic/hyperonic counterparts. (c) For neutron stars with canonical masses of around $1.4M_\odot$ we find a strong reduction of the radius of about $\leq 2.5$ km. The most compact stars, in this case, are those for which the coupling $R_{\sigma\Delta}$ is maximal. This reduction may help to achieve a better agreement of the theoretical model parameters of neutron stars with observations. Indeed the models with hyperons only produce $R = 13.9$ km for a $M = 1.4M_\odot$ model star, which is close to the upper range of radii (14 km) inferred in Refs. [88,90,91]. But it fails to satisfy the 13.2 km upper bound obtained in Refs. [89,92]. However, if $\Delta$'s are included and the coupling constants are chosen such that $R_{\sigma\Delta} \geq R_{\omega\Delta}$, the radius of the $M = 1.4M_\odot$ model is sufficiently reduced so that the latter constrained is satisfied too.

The trends discussed above can also be seen in Fig. 4. One sees that for the PKO3 parametrization $\Delta$'s appear already for $R_{\omega\Delta} - R_{\sigma\Delta} = -0.20$ irrespective of the value of $R_{\omega\Delta}$, while for the DD-ME2 parametrization $\Delta$'s are absent when $R_{\omega\Delta} - R_{\sigma\Delta} \leq -0.10$. This can be traced back to the differences in the isoscalar and isovector sectors of the *nucleonic CDF* models [39], as it is the nucleonic CDF model that determines the critical density of $\Delta$.

We have also examined the dependence of the compact star properties on the isovector meson–$\Delta$ coupling by setting $V_\Delta = V_N$ and $R_{\omega\Delta} = 1.1$ while varying $R_{\rho(\pi)\Delta}$ in the range $[0; 3]$. (We recall that the $V_\Delta(\rho_0)$-potential is independent of $R_{\rho(\pi)\Delta}$.) We find that modifications of the isovector couplings change the critical densities of delta isobars (for example, an increase $\simeq 0.04$ fm$^{-3}$ for $\Delta^-$ is observed over the entire range), which changes the particle fractions. Nevertheless, the maximum-star mass is insensitive to changes in $R_{\rho(\pi)\Delta}$. Indeed, varying $R_{\rho(\pi)\Delta}$ within the bounds mentioned just above decreases the maximum mass by only about $0.02M_\odot$ for both parametrizations. The radii are almost unchanged for the maximum-mass configurations, while they increase by about 0.3 km for canonical $1.4M_\odot$ neutron stars. This is because (a) the energy and pressure densities are dominated by the isoscalar channels and (b) the isovector couplings vanish exponentially at large densities in the present model. We conclude that there are no significant changes in stellar parameters associated with the variations of the isovector meson–$\Delta$ coupling.

## 4. Summary and conclusions

In this work, we have studied models of stellar matter which contain the full baryon octet and the delta decuplet within the CDF theory. We have used a class of models of CDF which feature density-dependent meson–baryon couplings. The meson–$\Delta$ coupling constants cannot be unambiguously constrained with the available empirical data. Therefore we have conducted a parameter study which included assumptions about the strength of the $\Delta$ potential in nuclear matter and a variation of couplings of the $\Delta$'s to mesons with strength close to that for nucleons. Our results indicate that $\Delta$ isobars may indeed appear in dense nuclear matter for a wide range of meson–$\Delta$ coupling constants.

We find that the appearance of $\Delta$'s softens the EoS in the low to intermediate-density region and stiffens it at high densities. This has two important effects on the global parameters of neutron stars: firstly, the maximum mass of a compact star increases by a small amount. Because the hypernuclear CDF parametrizations, employed in this work, satisfy the $2M_\odot$ maximum mass constraint, the inclusion of $\Delta$'s affect this feature only mildly. Secondly, and more importantly, the radius of a compact star decreases considerably, by about 2 km, for stars with a canonical mass of around $1.4M_\odot$ once $\Delta$'s are included.

We argued above that $\Delta$'s may also have a significant effect on the thermal evolution of compact stars, because they lead to changes in the particle concentration, which changes the thresholds and efficiency of the nucleonic and hyperonic DU processes. Furthermore, $\Delta^-$'s would contribute to the emissivity of the star via the DU process $\Delta^- \to \Lambda + e^- + \bar{\nu}_e$, which has an efficiency comparable to that of the nucleonic counterparts [33]. This process requires coexistence of $\Delta^-$'s and $\Lambda$'s which occurs in stellar models with $M \geq 1.5M_\odot$. Therefore, a natural extension of the present work would be to simulate the cooling of neutron stars containing $\Delta$'s in their centers.

## Acknowledgements

J.L. acknowledges the support by the Humboldt Foundation. A.S. is supported by the Deutsche Forschungsgemeinschaft (Grant No. SE 1836/4-1). The support from European COST Actions "NewCompStar" (MP1304) and "PHAROS" (CA16214) and the LOEWE-Program of Helmholtz International Center for FAIR of the State of Hesse (Germany) is gratefully acknowledged. F.W. is supported by the National Science Foundation (USA) under Grants PHY-1411708 and PHY-1714068.

## References

[1] N.K. Glendenning, Compact Stars: Nuclear Physics, Particle Physics, and General Relativity, Astronomy and Astrophysics Library, Springer, 1997.
[2] F. Weber, Pulsars as Astrophysical Laboratories for Nuclear and Particle Physics, Institute of Physics, Bristol, 1999.
[3] J.M. Lattimer, M. Prakash, Science 304 (2004) 536–542.
[4] F. Weber, R. Negreiros, P. Rosenfield, M. Stejner, Prog. Part. Nucl. Phys. 59 (2007) 94–113.
[5] A. Sedrakian, Prog. Part. Nucl. Phys. 58 (2007) 168–246.
[6] M. Oertel, M. Hempel, T. Klähn, S. Typel, Rev. Mod. Phys. 89 (2017) 015007.
[7] V.A. Ambartsumyan, G.S. Saakyan, Sov. Astron. 4 (1960) 187.
[8] V.R. Pandharipande, Nucl. Phys. A 178 (1971) 123–144.
[9] N.K. Glendenning, Astrophys. J. 293 (1985) 470–493.
[10] N.K. Glendenning, S.A. Moszkowski, Phys. Rev. Lett. 67 (1991) 2414–2417.
[11] J. Schaffner, C.B. Dover, A. Gal, C. Greiner, D.J. Millener, H. Stocker, Ann. Phys. 235 (1994) 35–76.
[12] H. Huber, F. Weber, M.K. Weigel, C. Schaab, Int. J. Mod. Phys. E 7 (1998) 301–339.
[13] E. Massot, J. Margueron, G. Chanfray, Europhys. Lett. 97 (2012) 39002.
[14] I. Bednarek, P. Haensel, J. Zdunik, M. Bejger, R. Mańka, Astron. Astrophys. 543 (2012) A157.
[15] S. Weissenborn, D. Chatterjee, J. Schaffner-Bielich, Nucl. Phys. A 881 (2012) 62–77.
[16] S. Weissenborn, D. Chatterjee, J. Schaffner-Bielich, Phys. Rev. C 85 (2012) 065802.
[17] T. Katayama, T. Miyatsu, K. Saito, Astrophys. J. Suppl. Ser. 203 (2012) 22.
[18] G. Colucci, A. Sedrakian, Phys. Rev. C 87 (2013) 055806.
[19] E. van Dalen, G. Colucci, A. Sedrakian, Phys. Lett. B 734 (2014) 383–387.
[20] D.L. Whittenbury, J.D. Carroll, A.W. Thomas, K. Tsushima, J.R. Stone, Phys. Rev. C 89 (2014) 065801.
[21] T. Katayama, K. Saito, Phys. Lett. B 747 (2015) 43–47.
[22] R.O. Gomes, V. Dexheimer, S. Schramm, C.A.Z. Vasconcellos, Astrophys. J. 808 (2015) 8.
[23] M. Oertel, C. Providência, F. Gulminelli, A.R. Raduta, J. Phys. G 42 (2015) 075202.
[24] K.A. Maslov, E.E. Kolomeitsev, D.N. Voskresensky, Phys. Lett. B 748 (2015) 369–375.
[25] L. Tolos, M. Centelles, A. Ramos, Astrophys. J. 834 (2017) 3.
[26] M. Fortin, S.S. Avancini, C. Providência, I. Vidaña, Phys. Rev. C 95 (2017) 065803.
[27] M. Marques, M. Oertel, M. Hempel, J. Novak, Phys. Rev. C 96 (2017) 045806.
[28] W. Spinella, Ph.D. thesis, Claremont Graduate University/San Diego State University, 2017.
[29] E.E. Kolomeitsev, K.A. Maslov, D.N. Voskresensky, Nucl. Phys. A 961 (2017) 106–141.
[30] A.R. Raduta, A. Sedrakian, F. Weber, Mon. Not. R. Astron. Soc. 475 (2018) 4347.
[31] R.F. Sawyer, Astrophys. J. 176 (1972) 205.
[32] J. Boguta, Phys. Lett. B 109 (1982) 251–254.
[33] M. Prakash, M. Prakash, J.M. Lattimer, C. Pethick, Astrophys. J. 390 (1992) L77–L80.
[34] Y. Chen, Y. Yuan, Y. Liu, Phys. Rev. C 79 (2009) 055802.
[35] T. Schürhoff, S. Schramm, V. Dexheimer, Astrophys. J. 724 (2010) L74.
[36] A. Lavagno, Phys. Rev. C 81 (2010) 044909.
[37] A. Drago, A. Lavagno, G. Pagliara, D. Pigato, Phys. Rev. C 90 (2014) 065809.
[38] A. Drago, A. Lavagno, G. Pagliara, Phys. Rev. D 89 (2014) 043014.
[39] B.-J. Cai, F.J. Fattoyev, B.-A. Li, W.G. Newton, Phys. Rev. C 92 (2015) 015802.
[40] A. Drago, A. Lavagno, G. Pagliara, D. Pigato, Eur. Phys. J. A 52 (2016) 40.
[41] Z.-Y. Zhu, A. Li, J.-N. Hu, H. Sagawa, Phys. Rev. C 94 (2016) 045803.
[42] A.B. Migdal, E.E. Saperstein, M.A. Troitsky, D.N. Voskresensky, Phys. Rep. 192 (1990) 179–437.
[43] T. Herbert, K. Wehrberger, F. Beck, Nucl. Phys. A 541 (1992) 699–713.
[44] C.L. Korpa, M.F.M. Lutz, F. Riek, Phys. Rev. C 80 (2009) 024901.
[45] S. Fritsch, N. Kaiser, W. Weise, Nucl. Phys. A 750 (2005) 259–293.
[46] P. Haensel, J.L. Zdunik, R. Schaefer, Astron. Astrophys. 160 (1986) 121–128.
[47] H. Heiselberg, C.J. Pethick, E.F. Staubo, Phys. Rev. Lett. 70 (1993) 1355–1359.
[48] S.K. Ghosh, S.C. Phatak, P.K. Sahu, Z. Phys. A 352 (1995) 457–466.
[49] A. Drago, A. Lavagno, Phys. Lett. B 511 (2001) 229–234.
[50] G.F. Burgio, M. Baldo, P.K. Sahu, H.-J. Schulze, Phys. Rev. C 66 (2002) 025802.
[51] F. Weber, Prog. Part. Nucl. Phys. 54 (2005) 193–288.
[52] M. Alford, M. Braby, M. Paris, S. Reddy, Astrophys. J. 629 (2005) 969.
[53] N.D. Ippolito, M. Ruggieri, D.H. Rischke, A. Sedrakian, F. Weber, Phys. Rev. D 77 (2008) 023004.
[54] V.A. Dexheimer, S. Schramm, Phys. Rev. C 81 (2010) 045201.
[55] L. Bonanno, A. Sedrakian, Astron. Astrophys. 539 (2012) A16.
[56] K. Masuda, T. Hatsuda, T. Takatsuka, Astrophys. J. 764 (2013) 12.
[57] M. Orsaria, H. Rodrigues, F. Weber, G.A. Contrera, Phys. Rev. C 89 (2014) 015806.
[58] T. Kojo, Eur. Phys. J. A 52 (2016) 51.
[59] W.M. Spinella, F. Weber, G.A. Contrera, M.G. Orsaria, Eur. Phys. J. A 52 (2016) 1–12.
[60] K. Fukushima, T. Kojo, Astrophys. J. 817 (2016) 180.
[61] I.F. Ranea-Sandoval, M.G. Orsaria, S. Han, F. Weber, W.M. Spinella, Phys. Rev. C 96 (2017) 065807.
[62] A. Sedrakian, EPJ Web Conf. 164 (2017) 01009.
[63] M. Alford, A. Sedrakian, Phys. Rev. Lett. 119 (2017) 161104.
[64] D.E. Alvarez-Castillo, D.B. Blaschke, Phys. Rev. C 96 (2017) 045809.
[65] D. Blaschke, N. Chamel, arXiv:1803.01836 [astro-ph].
[66] V. Pascalutsa, M. Vanderhaeghen, S.N. Yang, Phys. Rep. 437 (2007) 125–232.
[67] A. Bouyssy, J.-F. Mathiot, N. Van Giai, S. Marcos, Phys. Rev. C 36 (1987) 380–401.
[68] P. Ring, Prog. Part. Nucl. Phys. 37 (1996) 193–263.
[69] B.D. Serot, J.D. Walecka, Int. J. Mod. Phys. E 6 (1997) 515–631.
[70] W.-H. Long, N. Van Giai, J. Meng, Phys. Lett. B 640 (2006) 150–154.
[71] J.J. Li, W.H. Long, A. Sedrakian, arXiv:1801.07084 [astro-ph].
[72] R.C. Tolman, Phys. Rev. 55 (1939) 364–373.
[73] J.R. Oppenheimer, G.M. Volkoff, Phys. Rev. 55 (1939) 374–381.
[74] G. Baym, C. Pethick, P. Sutherland, Astrophys. J. 170 (1971) 299.
[75] G. Baym, H.A. Bethe, C.J. Pethick, Nucl. Phys. A 175 (1971) 225–271.
[76] J.J. de Swart, Rev. Mod. Phys. 35 (1963) 916–939.
[77] J. Mareš, E. Friedman, A. Gal, B.K. Jennings, Nucl. Phys. A 594 (1995) 311–324.
[78] K. Wehrberger, C. Bedau, F. Beck, Nucl. Phys. A 504 (1989) 797–817.
[79] J.S. O'Connell, R.M. Sealock, Phys. Rev. C 42 (1990) 2290–2294.

[80] W.M. Alberico, G. Gervino, A. Lavagno, Phys. Lett. B 321 (1994) 177–182.
[81] S.X. Nakamura, T. Sato, T.-S.H. Lee, B. Szczerbinska, K. Kubodera, Phys. Rev. C 81 (2010) 035502.
[82] G. Ferini, M. Colonna, T. Gaitanos, M. Di Toro, Nucl. Phys. A 762 (2005) 147–166.
[83] W.-M. Guo, G.-C. Yong, W. Zuo, Phys. Rev. C 92 (2015) 054619.
[84] M.D. Cozma, Phys. Lett. B 753 (2016) 166–172.
[85] W. Long, H. Sagawa, J. Meng, N. Van Giai, Europhys. Lett. 82 (2008) 12001.
[86] G.A. Lalazissis, T. Nikšić, D. Vretenar, P. Ring, Phys. Rev. C 71 (2005) 024312.
[87] J. Antoniadis, P.C.C. Freire, N. Wex, T.M. Tauris, R.S. Lynch, et al., Science 340 (2013) 6131.
[88] K. Hebeler, J.M. Lattimer, C.J. Pethick, A. Schwenk, Astrophys. J. 773 (2013) 11.
[89] J.M. Lattimer, A.W. Steiner, Eur. Phys. J. A 50 (2014) 40.
[90] A. Steiner, C. Heinke, S. Bogdanov, C. Li, W. Ho, A. Bahramian, S. Han, Mon. Not. R. Astron. Soc. 476 (2018) 421.
[91] F.J. Fattoyev, J. Piekarewicz, C.J. Horowitz, Phys. Rev. Lett. 120 (2018) 172702.
[92] J.M. Lattimer, Y. Lim, Astrophys. J. 771 (2013) 51.